Structure-Based Design on the Way to New Anti-Infectives

Hirsch, Anna K.H.

Published in:
Ideas in Chemistry and Molecular Sciences: Where Chemistry Meets Life

Publication date:
2010

7
Structure-Based Design on the Way to New Anti-Infectives

Anna Katharina Herta Hirsch

7.1
Introduction

With an estimated 300–500 million new infections and three million deaths annually, malaria and tuberculosis undoubtedly still pose a major health concern [1]. The need for the development of novel therapeutic approaches is ever-growing in light of the emergence of multi-drug-resistant parasites [2]. How can a new drug be identified?

First, a lead compound, that is, a molecule with a promising biological activity that does not yet fulfill all the requirements but represents the starting point on the way to a new drug, has to be identified. A number of different strategies exist to achieve this goal:

- *High-throughput screening* (HTS) of a large library of small molecules is of particular interest in cases in which no structural information or characterization of the biological target is available. The majority of lead compounds still comes from hits identified by HTS [3].
- *Virtual screening* has established itself as an alternative or complementary approach to classical HTS. Potentially active and/or drug-like compounds are selected from a library of compounds, using elaborate docking and scoring functions [4].
- C*ombinatorial chemistry* is useful for the formation of large, small-molecule libraries. However, this approach is less effective for generating a great deal of structural diversity.
- *Nature* can be of help by providing a rich and diverse source of structural inspiration [5]. The scaffold of a natural product, displaying interesting biological properties, could be developed into a new drug.
- *Structure-based design*, a comparatively new field, has established itself in pharmaceutical research as a valuable alternative to traditional screening; the X-ray crystal structure of a target enzyme is used as a basis for lead compound identification and optimization. The increasing number of leads, identified and/or optimized using this rational approach, used for the development of new drugs illustrates

Ideas in Chemistry and Molecular Sciences: Where Chemistry Meets Life. Edited by Bruno Pignataro

ISBN: 978-3-527-32541-2

this fact [6]. Until now, this strategy has been mainly used in the later stages of lead optimization.

The last mentioned strategy will be employed for the purposes of this project. The aim of this approach is to identify synthetically accessible target molecules, with optimal stereoelectronic properties that are complementary to the binding site of the target enzyme and show minimal or no repulsive interactions when complexed to the enzyme. The identification of promising leads is aided by the medicinal chemist's understanding of molecular recognition. While hydrophobic interactions between a lead and an enzyme are the main driving force for complexation, H-bonding interactions account for selectivity (Figure 7.1). Later stages of drug development are not the subject of this chapter.

To determine the biological activity of a potential lead compound, a new biological target [7], that is, an enzyme or receptor that upon interference by the ligand/drug has an impact on the disease causing pathogen in the desired way, has to be identified. In an ideal case, the target is essential for the pathogen and not present in humans, thereby precluding any selectivity issues. Isoprenoids are an essential class of natural products, requiring the essential precursors isopentenyl diphosphate (IPP, **1**) and dimethylallyl diphosphate (DMAPP, **2**) for their biosynthesis (Scheme 7.1). Until recently, only one route to the universal isoprenoid precursors was known, the so-called mevalonate pathway, using acetyl-coenzyme A as the only building block [8]. A completely distinct alternative to this well-established biosynthetic route, now known as the *nonmevalonate pathway*, was discovered in the early 1990s, starting from pyruvate (**3**) and glyceraldehyde 3-phosphate (**4**) [9]. Interestingly, this biosynthetic pathway is exclusively used by a number of pathogens such as the malarial parasite *Plasmodium falciparum* and the tuberculosis-causing *Mycobacterium tuberculosis* and not by higher eukaryotes (e.g., humans), which means that inhibition of the constituent enzymes of the nonmevalonate pathway affects and kills only the parasites, leaving the patient untouched (Scheme 7.1). Thus, this pathway has provided a rich source of new, highly attractive drug targets.

To illustrate the use of a structure-based design cycle, the development of the first inhibitors of the kinase IspE of the nonmevalonate pathway is described below, constituting a novel approach toward anti-infectives. First, the biosynthetic pathway

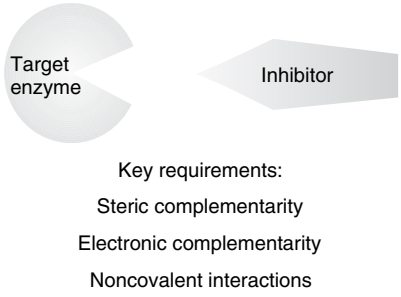

Figure 7.1 Schematic representation of structure-based inhibitor design.

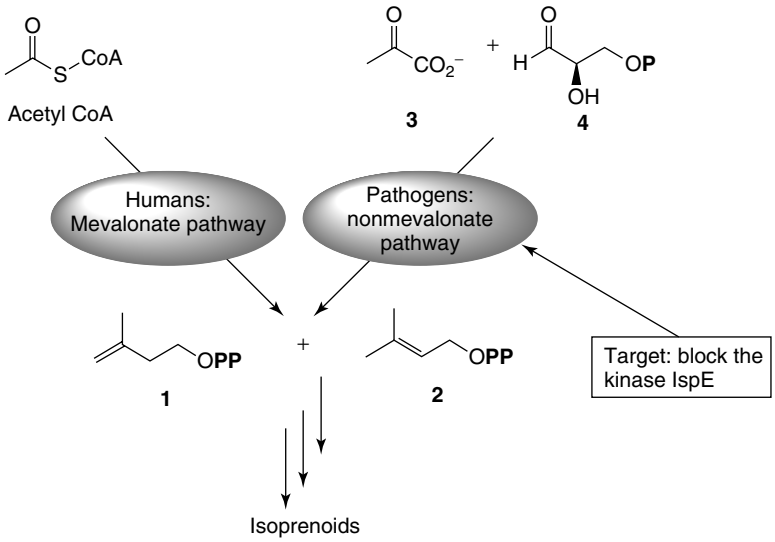

Scheme 7.1 Schematic representation of the biosynthesis of the isoprenoid precursors IPP (**1**) and DMAPP (**2**). **P** = phosphate group.

is briefly presented with an overview of the known inhibitors of the constituent enzymes. Subsequently, the chosen target, the kinase IspE, is introduced and its structure is discussed in some detail. This will provide the basis for the rationale of the design of the first-generation inhibitors. Second, the active site is explored by showing the possibility of applying concepts from supramolecular chemistry to an enzymatic context. Finally, the development of water-soluble inhibitors is described with the aim of obtaining an X-ray cocrystal structure to verify the proposed binding mode.

7.2
Isoprenoids and the Nonmevalonate Pathway

There are more than 35 000 known isoprenoids, which fulfill a myriad of important biological functions. Despite their striking structural diversity, all isoprenoids are biosynthesized from the two simple five-carbon building blocks **1** and **2** (Scheme 7.1). This concept is also known as the *isoprene rule* [10]. The nonmevalonate pathway starts with the head-to-tail condensation of the two- and three-carbon precursors **3** and **4**. A total of seven enzymes catalyze the conversion of these starting materials into the essential isoprenoid precursors **1** and **2**. Fosmidomycin, an inhibitor of the second enzyme of the pathway (IspC), has been shown to cure malaria in rodents, thereby validating the constituent enzymes as drug targets [11]. This finding triggered research efforts aimed at the elucidation of the structures

and mechanisms of the participating enzymes. As a result, detailed structural and mechanistic data exist for most enzymes [12], setting the stage for lead generation by structure-based design. A number of enzymes of the nonmevalonate pathway have been chosen as targets to achieve this goal. The rather hydrophilic nature of the active sites renders the development of low-molecular-weight inhibitors challenging. Thus, it comes as no surprise that the few reported inhibitors either bear phosphate or phosphonate groups or display rather modest inhibition (Table 7.1) [13].

7.2.1
4-Diphosphocytidyl-2*C*-methyl-D-erythritol Kinase (IspE)

The absence of known inhibitors, the fact that the kinase IspE belongs to the nonmevalonate pathway, and the availability of an X-ray crystal structure make the fourth enzyme of the pathway an ideal target for rational design of potent, drug-like inhibitors without the use of the problematic phosphate or phosphonate moieties. IspE (EC 2.7.1.148) employs adenosine 5′-triphosphate (ATP) and Mg^{2+} cations for the phosphorylation of the C(2)-hydroxyl group of 4-diphosphocytidyl-2*C*-methyl-D-erythritol (**5**) to afford 4-diphosphocytidyl-2*C*-methyl-D-erythritol 2-phosphate (**6**, Scheme 7.2) [18].

This central reaction is the only ATP-dependent step of the whole biosynthetic pathway. Sequence comparisons have shown that IspE belongs to the galactose/homoserine/mevalonate/phosphomevalonate (GHMP) kinase superfamily [19].

7.2.2
Structure of IspE

In 2003, the first crystal structures of IspE from *Thermus thermophilus* and *Escherichia coli* were solved, of the apoenzyme and of a ternary complex, respectively [20, 21]. Recently, the crystal structure of *Aquifex aeolicus* IspE was solved as a complex with a number of natural ligands [22], a synthetic substrate mimic [22], and synthetic cytidine [23] as well as cytosine (Section 7.4) [24] derivatives. To date, no crystal structure is available for IspE from a pathogen, for example, *M. tuberculosis* or *P. falciparum*. IspE generally crystallizes as a homodimer with each monomer displaying the characteristic two-domain fold of the GHMP kinase superfamily that consists of an ATP- and a substrate-binding domain. The dimer clasps around a solvent-filled channel, featuring two active sites at either end (Figure 7.2).

7.2.3
Active Site of IspE

The active site of *E. coli* IspE was used for modeling. It can be divided into three main pockets: the ATP-, the cytidine 5′-diphosphate (CDP)-, and the methylerythritol (ME)-binding pockets. Molecular modeling, using the program MOLOC

Table 7.1 Known inhibitors of enzymes of the nonmevalonate pathway.

Enzyme	Inhibitors	Inhibition
DXS	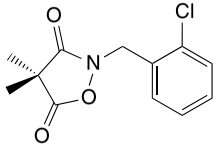 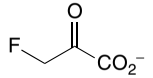	$IC_{50} = 0.08$ mM [14]
IspC	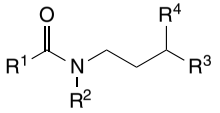 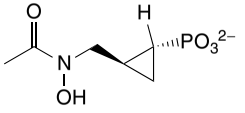 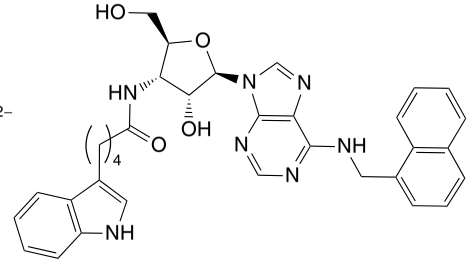	$K_i = 0.9$ nM [15]
IspE	No known inhibitors at the onset of the present design cycle	
IspF	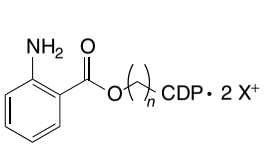 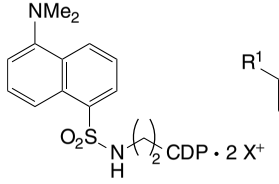 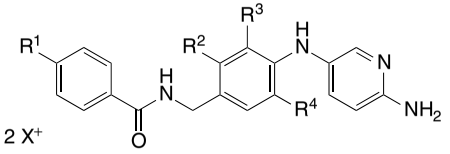	$IC_{50} = 0.45$ mM [16]
IPP isomerase	Substrate and transition-state analogues / Mechanism-based inhibitors	$K_i = 0.011$ μM [17]

The inhibition of the best inhibitor is given. CDP = cytidine 5′-diphosphate; DXS and IspF: first and fifth enzyme of the nonmevalonate pathway, respectively; IC_{50} = concentration of inhibitor at which 50% maximum initial velocity is observed; K_i = inhibition constant.

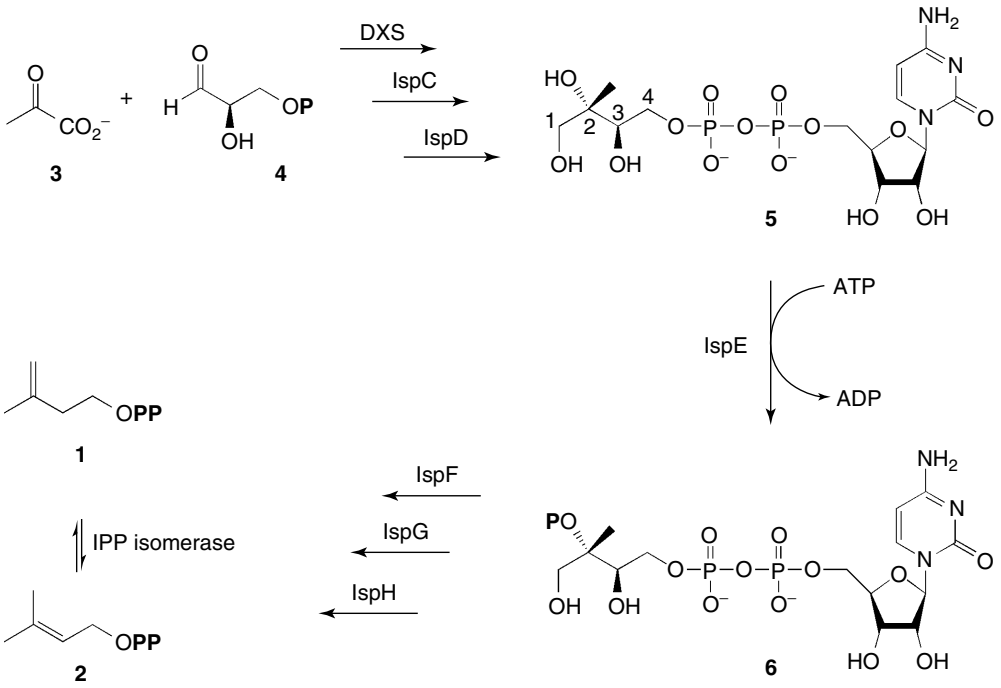

Scheme 7.2 Simplified version of the nonmevalonate pathway.

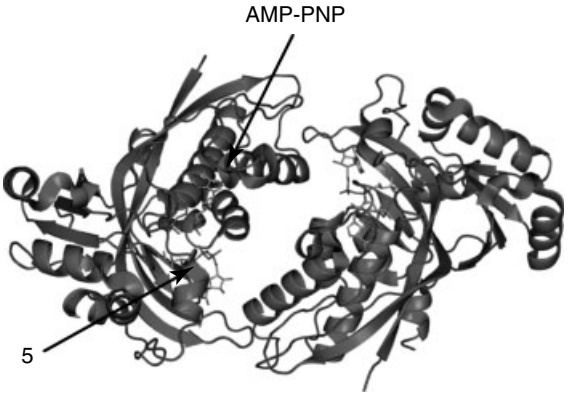

Figure 7.2 Schematic representation of the ternary complex of *E. coli* IspE, 5′-adenyl-β,γ-amidotriphosphate (AMP-PNP) and the substrate **5**, cocrystallized as a homodimer (Protein Data Bank (PDB) code: 1OJ4) [20].

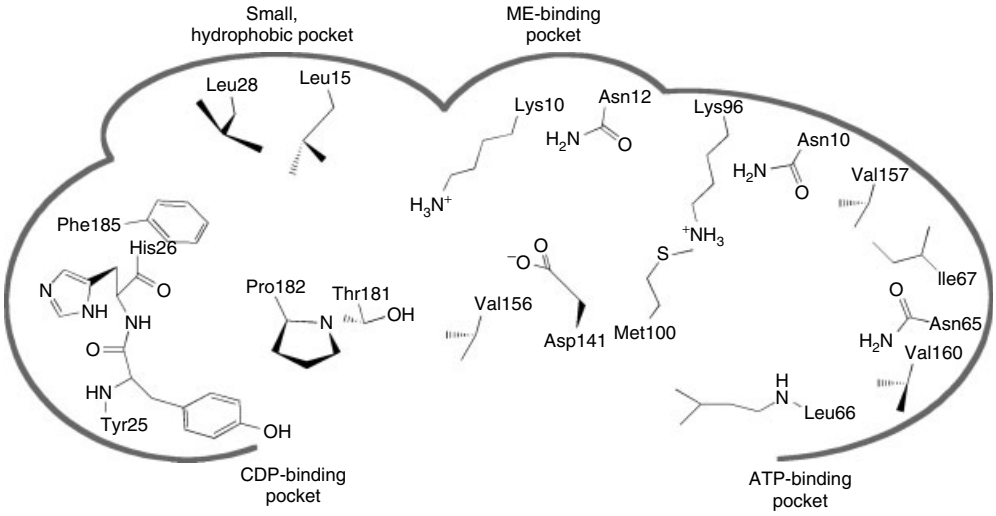

Figure 7.3 Schematic representation of the four pockets of the active site of *E. coli* IspE. The residues of the glycine-rich loop were omitted for clarity.

[25], revealed that an additional small, hydrophobic pocket lies adjacent to the CDP-binding site (Figure 7.3).

The ATP-binding pocket features a glycine-rich phosphate-binding loop, typically displaying an adjacent positively charged N terminus of an α helix [20]. The adenine moiety is accommodated in a hydrophobic cleft lined by Val57, Val60, Leu66, Ile67, Lys96, and Met100. Numerous hydrophobic contacts offered by this pocket certainly make a large contribution to the binding enthalpy, as predicted by MOLOC. Additional stabilization is derived from a network of H bonds to the nucleobase moiety. The ribose moiety of 5′-adenyl-β,γ-amidotriphosphate (AMP-PNP) is solvent-exposed and does not show any contacts with the protein.

The CDP-binding pocket accommodates the cytosine moiety in a π sandwich, consisting of the side chains of Tyr25 and Phe18 held in place by – stacking interactions. The ribose moiety benefits from stabilization by a pseudo-π sandwich that is composed of the aromatic side chain of Tyr25 and the aliphatic Pro182. A *pseudo-π sandwich* can be defined as a π sandwich, in which one of the two aromatic rings is replaced by an aliphatic ring. His26 is a key residue for the recognition of cytosine, which involves a total of three H-bonding interactions. The ribose and phosphate groups are stabilized by a number of solvent-mediated interactions and a H bond from the side chain of Tyr25 (Figure 7.4).

IspE was shown to have high substrate specificity [21]. Hence, the cytosine moiety must play a key role in substrate recognition and thus selectivity, providing the starting point for the structure-based design of the first-generation inhibitors (Section 7.3).

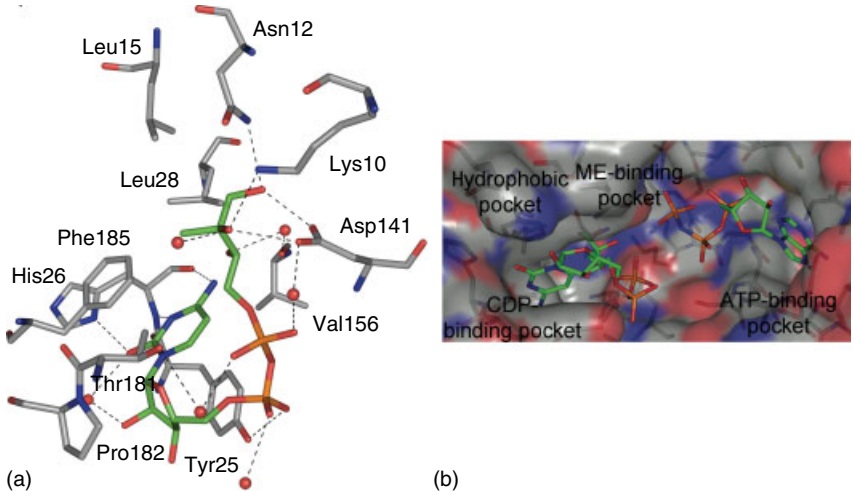

Figure 7.4 (a) CDP- and ME-binding and the small, hydrophobic pockets of *E. coli* IspE. (b) Active site of *E. coli* IspE (PDB code: 1OJ4) [20]. Color code: protein skeleton: C: gray; skeleton of **5**: C: green; O: red; N: blue; P: orange.

7.3 Targeting the CDP-Binding Pocket of IspE

7.3.1 Design

Careful examination of the active site revealed the CDP-binding pocket to be more attractive as a target for inhibitor design than the other binding pockets for a number of reasons. A perfect setup for a double π sandwich and other recognition features should endow potential inhibitors with higher selectivity. Furthermore, given the myriad of proteins that use ATP as a cofactor, inhibitors designed to target the ATP-binding pocket bear a high risk of selectivity issues. Given that neither substrate nor cofactor bind to the adjacent, hydrophobic pocket, presumably, both affinity and selectivity could be gained by occupying it. As this small cavity lies adjacent to the CDP-binding pocket, potential inhibitors should be designed to occupy both the CDP-binding pocket and the newly discovered subpocket, leaving the hydrophilic ME- as well as the ATP-binding pockets unoccupied.

In a first round of design, cytosine was chosen as a central scaffold to position potential inhibitors in the CDP-binding pocket. According to modeling, the nucleobase moiety was predicted to be sandwiched between Tyr25 and Phe185. By analogy to the natural substrate **5**, the cytosine moiety was postulated to be able to form H bonds to His26. It was concluded that the central platform should be decorated with a suitable ribose analogue at the N(1) position, which should be held in place by the pseudo-π sandwich and a vector designed such that its

substituent would be placed in the hydrophobic subpocket. If this were to be achieved, numerous hydrophobic interactions would result. By connecting the linker to the C(5) position, it should serve to address the catalytically essential residues Lys10 and Asp141. Because of the modular design, the different components, that is the ribose analogue, the vector, and the central scaffold, should be easy to vary and optimize (Figure 7.5a).

7.3.1.1 **Possible Ribose Analogues**

As ribose analogues, both heteroalicyclic and aromatic rings can be envisaged to fill the space provided by the pseudo-π sandwich (Figure 7.5b, compounds of type **7** and **8**). Introduction of a saturated ring featuring a sulfur atom, for example, a tetrahydrothiophenyl ring, presumably would enable an additional sulfur–aromatic interaction with the phenolic ring of Tyr25 [27]. Modeling predicted both enantiomers of a tetrahydrothiophenyl derivative to bind with similar strength due to the conformational flexibility of five-membered rings. Four questions need to be answered regarding the choice of the ribose analogue: (i) Which is the ideal ring size? (ii) Is an aromatic or an aliphatic system favored? (iii) Are heteroatoms beneficial? (iv) Is a connecting methylene linker beneficial or detrimental to affinity?

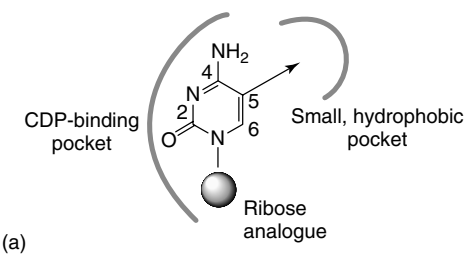

(a)

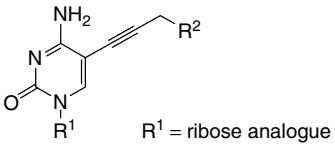

(c)

Inhibitor	R^2	clogP
(±)-**9**	Alicyclic amine	1.1 to 2.3
10	OH	1.2

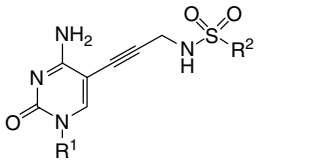

(b)

Inhibitor	R^1	clogP[a]
7	Saturated cyclic	0.3 to 1.0
8	Methylene bridged	–0.4 to 1.5

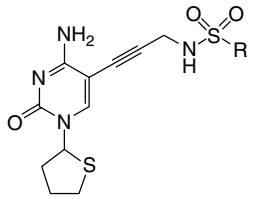

(d)

Inhibitor	R	clogP
(±)-**11**	Acyclic	0.3 to 2.0
(±)-**12**	Cyclic	–0.03 to 2.6

Figure 7.5 (a) Modular design of first-generation inhibitors. (b) Ribose analogues, (c) different vectors, and (d) sulfone substituents envisaged for first-generation inhibitors. [a]clogP values (calculated partitioning coefficient) were calculated with the program ACD/LogP [26]. The tetrahydrothiophenyl and the tetrahydrofuranyl derivatives of type **7** and **8**, respectively, are chiral.

7.3.1.2 Design of the Vector

For the vector, a propargylic sulfonamide substituent at the C(5) position of cytosine was envisaged, which displays three attractive features. First, the alkyne ensures a certain rigidity and linearity. Second, N-substituted sulfonamides are known to prefer a conformation in which the lone pair of the nitrogen atom bisects the O–S–O angle, resulting in a staggered arrangement [28]. In its preferred conformation, the sulfonamide is expected to form ionic H bonds to the side chains of Lys10 and Asp141. Finally, small complementary sulfone substituents (R^2 = Et, Figure 7.5a), should orient directly into the subpocket. However, before this part of the vector is optimized (Section 7.3.4), the importance of the sulfonamide's contribution to affinity should be evaluated (Section 7.3.3).

An exemplary inhibitor of type **7** features a tetrahydrothiophenyl ring as a ribose mimic (R^1) and an ethyl group as a sulfone substituent (R^2) (Figure 7.5b). According to modeling, the ligand should benefit from H bonds to His26, Lys10, and Asp141 as well as from the postulated sulfur–aromatic interaction (Figure 7.6a). An overlay of the natural substrate **5** and the potential inhibitor showed the sulfone moiety to be almost perfectly superimposed with the C(2)-hydroxyl group that is to be phosphorylated (Figure 7.6b).

The synthesis of the first representative of the first-generation inhibitors was achieved using a convergent strategy based on the Sonogashira cross-coupling reaction [29, 30]. With the synthetic route in place, the optimization of both modules of the inhibitors could be initiated in parallel.

7.3.2 Optimization of the Ribose Analogue

It was envisaged to introduce a number of different ribose analogues (Figure 7.5b). Different ring types had to be tested: saturated, aromatic, or heteroaromatic rings, all of which should be directly attached to the N(1) of the nucleobase (ligands of type **7**). Furthermore, the influence of a connecting methylene group between N(1)

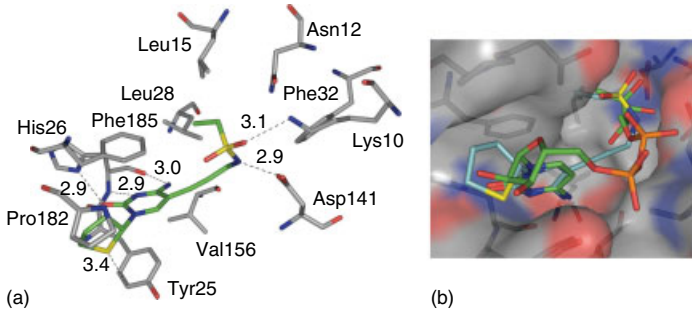

Figure 7.6 (a) MOLOC-generated molecular model of the exemplary inhibitor in the active site of *E. coli* IspE (PDB code: 1OJ4) [20]. (b) Superposition of the potential inhibitor and the natural substrate **5**. Color code: S: yellow; C skeleton of the inhibitor: cyan.

of cytosine and the ribose analogue needed to be evaluated both for aliphatic and (hetero-)aromatic substituents (compounds of type **8**). In addition, it was deemed important to test an acyclic ribose mimic, featuring an ester group. Replacement of the sulfur atom of the tetrahydrothiophenyl ring of the exemplary inhibitor by a methylene moiety to afford a cyclopentyl ring as a ribose analogue was expected to yield information on the postulated sulfur–aromatic interaction. Synthesis of this set of potential inhibitors was achieved using similar synthetic routes [24, 29].

Using the established photometric assay to determine the activity of potential inhibitors against IspE, the IC_{50} and K_i values for all new ligands were determined (Table 7.2) [24, 29, 31]. A competitive mechanism with respect to substrate binding was assigned to most ligands. In a few cases, however, a mixed competitive (K_{ic})–uncompetitive (K_{iu}) mode of inhibition was found. In agreement with the observation that small cytosine derivatives possess remarkably low water solubility [24], none of the inhibitors showed high water solubility, despite the low calculated partitioning coefficient (clogP) values (Figure 7.5b).

The results obtained are highly satisfactory: First, as no inhibitors of IspE had been described at the onset of this design cycle, obtaining the first active compounds with K_i values in the upper-nanomolar range constitutes an important achievement. Second, inhibition was possible in the absence of a phosphate or phosphonate group. The ligands described constitute the first example of potent, drug-like inhibitors of an enzyme of the nonmevalonate pathway. Furthermore, variation of the ribose mimic has a clear effect on affinity, that is, structure–activity relationships (SARs) could be observed. A methylene-bridged tetrahydrofuranyl ring is the poorest ribose substitute with a double-digit micromolar K_i value. Introduction of a methylene-bridged aromatic ring (benzyl) or an open alkyl chain bearing an ester moiety as a ribose mimic clearly also has a negative effect on affinity. However, it seems that a methylene-bridged ring is tolerated as long as it is not too bulky: the methylene-bridged cyclobutyl and pyrazolyl derivatives feature similar affinities to that of the inhibitor bearing a cyclopentyl ring directly attached to N(1) of cytosine. On the basis of the affinities, there does not seem to be any

Table 7.2 Inhibitory activities (*E. coli* IspE) of compounds of type **7** and **8**.

Ribose analogue	K_{ic} (μM)[a]
Tetrahydrothiophenyl	0.29 ± 0.1
Cyclopentyl	1.5 ± 0.2
Cyclobutylmethyl	1.5 ± 0.2
CH_2–3-pyrazolyl	1.6 ± 0.1
Benzyl	3.7 ± 0.5[b]
CH_2CO_2Et	4.2 ± 0.6[c]
CH_2–2-tetrahydrofuranyl	32.3 ± 2.8

[a] The IC_{50} values can be found in 24, 29, 30.
[b] Mixed inhibition: $K_{iu} = 23.5 \pm 7.1$ μM.
[c] Mixed inhibition: $K_{iu} = 21.6 \pm 6.2$ μM.

significant difference between a heteroaromatic ring such as pyrazolyl and the alicyclic cyclopentyl ring. However, if clogP values are taken into account, the latter inhibitor is significantly more lipophilic; hence, the resulting more favorable partitioning from the aqueous buffer into the less polar protein environment could partially account for its affinity. This implies that heteroatoms afford some affinity.

Finally, the tetrahydrothiophenyl ring is the best ribose mimic, affording the lowest K_i value. Presumably, its improved affinity could be ascribed to the favorable sulfur–aromatic interaction. This interaction was quantified when comparing the affinities of the tetrahydrothiophenyl derivative with an inhibitor bearing the same sulfone substituent (cyclopropyl) and a cyclopentyl ring as a ribose analogue. The affinity is lowered by a factor of five, corresponding to a free-enthalpy increase of $\Delta\Delta G_{300\ K} \approx 1\ kcal\,mol^{-1}$, in agreement with published data [27]. Both rings benefit from stabilization by the pseudo-π sandwich. Thus, the higher affinity could be explained by favorable interactions of the phenolic side chain and the sulfur atom of the sandwiched ring.

7.3.3
Importance of the Vector

Before optimizing the propargylic sulfonamide vector, its significance has to be confirmed. According to modeling, the sulfonamide group forms two H bonds to Lys10 and Asp141. To verify this prediction experimentally, four derivatives featuring modified vectors and established ribose analogues were designed and synthesized (Figure 7.5c): (i) The N-methylated derivative of the most potent inhibitor, featuring a cyclopropyl ring as sulfone substituent and a tetrahydrothiophenyl ring as ribose analogue, served to quantify the importance of the ionic H bond between the sulfonamide NH and the side chain of Asp141. (ii) Different propargyl amine derivatives [compounds of type (±)-**9**] as well as propargyl alcohol derivative **10** were envisaged to evaluate the effect of substituting the sulfonamide altogether. The set of target molecules were synthesized following similar routes [24].

Using the established enzymatic assay, the IC_{50} and K_i values of the potential inhibitors were determined [24, 29, 31]. N-methylation of the sulfonamide nitrogen atom clearly affected affinity, illustrating the importance of the postulated ionic H bond. Modeling showed the inhibitor to be still accommodated in the active site without any repulsive interactions but with one less H bond. Comparison with the most potent inhibitor enabled the quantification of the postulated ionic H bond, given that both ribose analogue and sulfone substituent remained unchanged. The inhibitory potency was reduced by a factor of nearly 10 upon N-methylation ($K_i = 2.5\ \mu M$); thus, a contribution of up to $\Delta\Delta G_{300\ K} = 1.3\ kcal\,mol^{-1}$ to the overall binding free enthalpy could be ascribed to this H bond alone (Figure 7.7a).

As expected, substitution of the sulfonamide moiety by heterocyclic amines led to a decrease in inhibitory potency. A piperidyl-substituted derivative maintains the highest affinity ($K_i = 4.7\ \mu M$). A possible explanation could be an ionic H bond between the side chain of Asp141 and the piperidinium residue (Figure 7.7b). According to modeling, the piperidinyl ring should be located at the entrance of the

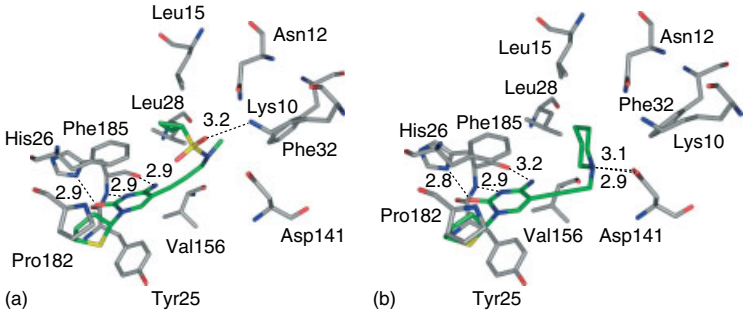

Figure 7.7 MOLOC-generated molecular model of (a) the N-methylated and (b) the piperidinyl-substituted inhibitors in the active site of *E. coli* IspE (PDB code: 1OJ4) [20]. Reproduced with permission from the Royal Society of Chemistry.

small, hydrophobic pocket. In this way, a number of hydrophobic interactions with the residues lining this cavity are still possible. A pyrrolidinyl-substituted derivative was proposed to bind in a similar manner, displaying fewer hydrophobic contacts because of its smaller ring. As a result, a decrease in binding affinity was observed ($K_i = 11.8\ \mu M$). The alcohol **10** shows very weak affinity for IspE; consequently, no K_i value could be determined. This observation could be explained by the lack of both a sulfonamide moiety and an alkyl substituent to benefit from potential interactions in the small, hydrophobic cavity.

In summary, important contributions of the sulfonamide moiety to the observed binding affinity were clearly confirmed through this set of derivatives. With the sulfonamide moiety validated as a good vector, the next logical step was therefore the optimization of the sulfone substituent R (Figure 7.5d).

7.3.4
Optimization of the Filling of the Small, Hydrophobic Pocket

Inspired by the finding that optimal volume occupancy can be an important contributor to affinity [32], the small, hydrophobic pocket of IspE was carefully examined. For this purpose, a series of derivatives of type (±)-**11** and (±)-**12** were designed, differing only in the sulfone substituent as shown in Figure 7.5d. By keeping the scaffold, the vector and the ribose analogue constant, the effects of different substituents on affinity should be directly comparable. The target molecules were readily synthesized [24]. The choice of substituents was guided by the predictions made by molecular modeling and a concept from conventional supramolecular chemistry – the "55% rule" – that was recently applied to enzymes for the first time [33].

7.3.4.1 The "55% Rule"

Investigation of the optimal volume occupancy of the cavity space confined by capsular synthetic receptors by Mecozzi and Rebek led to the "55% rule," stating

that the most stable inclusion complex forms if 55 ± 9% of the apolar space is occupied by the guest [34]. This concept holds true, from synthetic supramolecular chemistry [35]. Recently, Zürcher *et al.* applied it to the filling of a hydrophobic cavity in the active site of the antimalarial target plasmepsin II [33]. The van-der-Waals interactions in the cavity are not ideal at smaller packing coefficients (PCs). At higher PCs, however, large entropic losses, resulting from a decrease in the mobility of the binding partners, counteract enthalpic gains.

The small, hydrophobic pocket of *E. coli* IspE was estimated to be around 100 Å^3 by filling the pocket with a hydrocarbon network [34, 36]. Thus, the PCs were calculated for different target molecules, which guided their design.

7.3.4.2 Evaluation of Inhibitors Featuring Different Sulfone Substituents

A series of potential inhibitors were subjected to the enzymatic assay. The inhibitory activities as well as the calculated PCs for selected compounds are summarized in Table 7.3.

A number of derivatives prepared feature K_i values in the nanomolar range. In general, small alkyl chains with a maximum chain length of two carbon atoms or cyclic alkyl substituents up to a ring size of five are well suited to fill the cavity; hence, it is presumably more flexible on the sides than at its bottom. The three-membered ring seems to be ideal to fill this lipophilic pocket. A 2,2,2-trifluoroethyl group almost affords the same affinity as the most potent inhibitor (featuring a cyclopropyl ring)

Table 7.3 Inhibitory activities (*E. coli* IspE) and PCs of compounds of type (±)-**11** and (±)-**12**.

Sulfone substituent	K_{ic} (μM)	PC (%)
Cyclopropyl	0.29 ± 0.1	56
2,2,2-Trifluoroethyl	0.36 ± 0.1	n.d.
Isopropyl	0.52 ± 0.1	62
Cyclobutyl	0.56 ± 0	69
Ethyl	0.64 ± 0.1	45
Cyclopentyl	0.89 ± 0.1[a]	83
1,1,1-Trifluoromethyl	1.2 ± 0.3	n.d.
sec-Butyl	1.8 ± 0.3	n.d.
n-Hexyl	2.0 ± 0.3	107
Cyclohexyl	2.5 ± 0.4[b]	97
Methyl	2.6 ± 0.1	28
n-Butyl	8.0 ± 0.1	76
n-Propyl	8.2 ± 1.7[c]	61
Phenyl	16.3 ± 1.0	n.d.

[a] Mixed inhibition: K_{iu} = 19.0 ± 9.2 μM.
[b] Mixed inhibition: K_{iu} = 67.7 ± 35 μM.
[c] Mixed inhibition: K_{iu} = 27.3 ± 11 μM.
n.d. = not determined.

and is nearly twice as strong as the corresponding ethyl derivative (Figure 7.6a). The affinity of isopropyl- and cyclobutyl-substituted ligands is very similar to that of the ethyl-substituted derivative; however, the alkyl residues seem to be slightly too large for optimal volume occupancy, leading to a decrease in affinity. As the pocket is not properly filled by ligands with a smaller alkyl substituent (methyl), the binding affinity is reduced.

Evaluation of the set of derivatives in terms of their PCs showed binding affinity to correlate with volume occupancy: a cyclopropyl ring has a PC of 56% and the lowest K_i value ($K_i = 0.29$ µM, Figure 7.8a).

Lower (28% for methyl and 45% for ethyl substituents) or higher PCs (62% for isopropyl and 69% for cyclobutyl) are mirrored by weaker inhibition. A slight increase in size of the sulfone substituent – that is, extension of the ethyl substituent by one or two carbon atoms – led to a strong decrease in affinity. According to modeling, the *n*-propyl substituent might still fit into the cavity at the cost of adopting the energetically less favorable *gauche* conformation (PC 61%). The *n*-butyl substituent, however, cannot be accommodated by the pocket, even when contorted. Thus, the propargylic sulfonamide linker could equally well undergo a conformational change to direct this substituent out of the pocket into solvent-exposed space. Larger substituents (PC > 80%), such as cyclopentyl, cyclohexyl, or *n*-hexyl, were predicted to direct their alkyl substituents toward the opposite direction, that is, toward the solvent (Figure 7.8b).

The increased lipophilicity (cf. clogP values) and the resulting more favorable partitioning to the less polar protein environment from the aqueous buffer could explain the increased binding affinity.

In summary, by exploring the small, hydrophobic pocket, the affinity of the inhibitors was improved and another example for the application of the "55% rule" to an enzymatic context was provided.

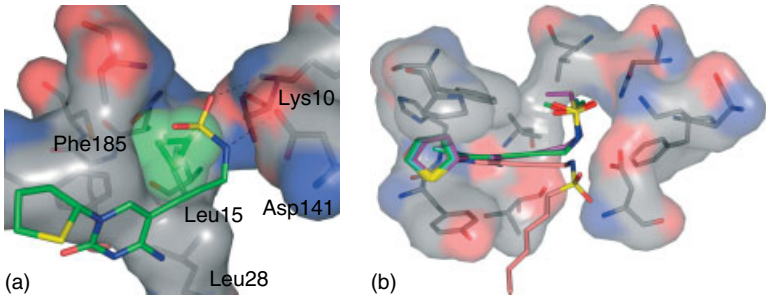

Figure 7.8 (a) van-der-Waals surfaces of the cyclopropyl ring of the most potent inhibitor of type (±)-**11** and the protein in the small, hydrophobic pocket. (b) MOLOC-generated molecular model of the alkyl-substituted inhibitors in the active site of *E. coli* IspE (PDB code: 1OJ4) [20]. Color code: C skeleton of the inhibitors: methyl, cyan; ethyl, magenta; *n*-propyl, green; *n*-hexyl, light pink.Reproduced with permission from the Royal Society of Chemistry.

7.3.5
Summary of the First-Generation Inhibitors

In conclusion, addressing the CDP-binding pocket was rewarded with the discovery of the first, potent, small-molecule inhibitors of IspE. The affinity could be improved through rational modifications of the lead compound, giving access to an extensive set of SARs; for the time being, they provide the only indication that the proposed binding mode is correct. X-ray-crystallographic studies had to be performed to validate this hypothesis (Section 7.4).

7.4
X-ray Cocrystal Structure Analysis

Efforts were undertaken to obtain a cocrystal structure of the first-generation inhibitors and IspE. The kinase is very sensitive to crystallization conditions; even traces of organic cosolvents are sufficient to preclude crystal growth. Presumably, because of the lack of water solubility of the first-generation inhibitors, no cocrystal structures could be obtained. Thus, a water-soluble derivative had to be designed (Section 7.4.1). Provided it resembled the structure of the inhibitors in hand, it could prove the binding mode of this class of compounds.

7.4.1
Design of Water-Soluble Inhibitors

Modeling as well as clogP values were used to guide the selection of promising target molecules (Figure 7.9).

To improve the water solubility of the first-generation inhibitors without a concomitant decrease in affinity, the sulfone substituent or the sulfonamide vector (target molecules of type (±)-**13**) or the ribose analogue (ligands of type **14**) could be modified. Given that modestly potent inhibitors could be cocrystallized (Section 7.2.2), the proposed series of target molecules looked promising as long as water solubility could be achieved. Two derivatives were obtained by varying

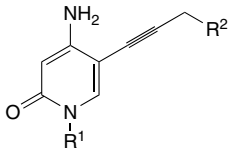

Inhibitor	R^1	R^2	clogP
(±)-**13**	2-Tetrahydrothiophenyl	Morpholinyl based	–0.49 to 0.9
14	Carboxylic-acid-based	Cyclopropyl	–0.6 to 0.4

Figure 7.9 Target molecules to improve the water solubility of the first-generation inhibitors.

the vector, whereas the remaining three resulted from a modification of the ribose analogue. Introduction of a carboxylic acid or the corresponding ester functionality, a morpholinyl, or an oxetanyl substituent should afford the desired property. Oxetanes, in particular, were recently described to endow compounds with improved physicochemical properties, namely, affording enhanced solubility and decreased lipophilicity [37].

7.4.2
Enzyme Assays of Inhibitors Designed to be Water Soluble

Among the six compounds specifically prepared to obtain water-soluble inhibitors, two (the morpholinyl-substituted sulfonamide ($K_i = 13.1\ \mu M$) and the oxetanyl derivative (compound **15**, Figure 7.10b, $K_i = 28.7\ \mu M$)) do not require addition of dimethyl sulfoxide as a cosolvent to perform the enzyme assay [24]. While the former still requires ethanol as a cosolvent, the latter is water soluble, setting the stage for X-ray crystallographic studies (Section 7.4.3).

Water solubility was achieved at the expense of potency: the affinity was decreased by nearly two orders of magnitude, when replacing the tetrahydrothiophenyl ring of the most potent inhibitor by the oxetanyl substituent of inhibitor **15**. Because of their poor affinities, only the IC_{50} values of the carboxylic acid derivatives were determined (upper micromolar range). The weak inhibitory potency of the morpholinyl derivative lacking the sulfonamide moiety could be explained by the bad match between the electronics of the morpholinyl moiety and the small, hydrophobic subpocket. Thus, introduction of an oxygen atom to the piperidinyl derivative of type (±)-**9** (Section 7.3.3), affording the corresponding morpholinyl-substituted ligand, resulted in a decrease in affinity by almost a factor of nine. A similar decrease in affinity was observed when changing the sulfone substituent from cyclohexyl (compound of type (±)-**12**) to morpholinyl. The poor affinity of the carboxylic acid derivatives could be attributed to the less than optimal ribose mimics.

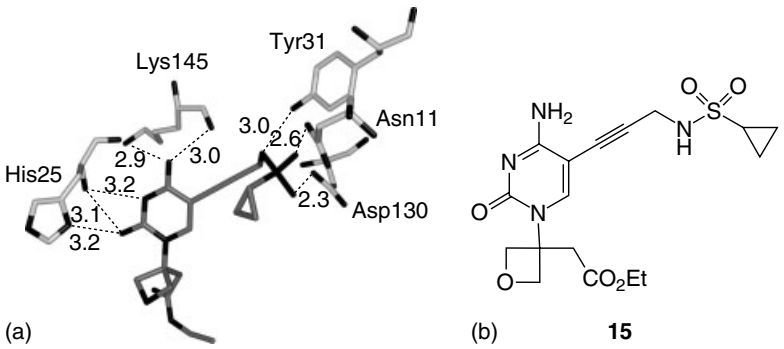

Figure 7.10 (a) Binding mode of inhibitor **15** in the CDP-binding pocket of active site B (PDB code: 2VF3) [24]. (b) Structure of compound **15**.

7.4.3 Structural Analysis

The structure of the oxetanyl derivative **15** in complex with *A. aeolicus* IspE was determined to 2.2 Å resolution (PDB code: 2VF3) [24]. Two molecules are present in the asymmetric unit, featuring ''active sites A and B.'' Evidence for the proposed binding mode of inhibitor **15** was provided by the cocrystal structure. The water-soluble ligand indeed binds in the CDP-binding pocket. As a result of the differences in amino-acid sequences of *A. aeolicus* and *E. coli* IspE [30], the sulfonamide and nucleobase moieties form somewhat different H-bonding patterns compared to those predicted by modeling. In particular, two additional H bonds stabilize the cytosine moiety of ligand **15** (Figure 7.10a). The cytosine moiety is engaged in four H bonds to the side chain and backbone amide of His25 in active site B. The amino group forms an additional H bond to the backbone amide C=O of Lys145. The cytosine ring is sandwiched by the side chains of Tyr24 and Tyr175 (= Phe185 in *E. coli* IspE). A network of H bonds to the side chains of Asn11, Tyr31, and Asp130 stabilizes the sulfonamide moiety (Figure 7.10a).

Although AMP was present in the crystallization conditions, the electron density observed in the glycine-rich loop of the ATP-binding pocket was incompatible with this compound. Modeling and refinement of the density as diphosphate proved successful. The latter unit forms numerous H bonds to the backbone-amide NH groups of the glycine-rich loop, in analogy to the diphosphate moiety of AMP-PNP in the crystal structure of the *E. coli* enzyme complex [20]. With one exception (Gly95), all the backbone-amide NH moieties of glycine residues of the loop are involved in H-bonding. The residues of the glycine-rich loop, which are not glycine, however, do not participate in H-bonding interactions with diphosphate. This underlines the importance of the presence of glycine residues in phosphate-binding pockets. Presumably, glycine is ideally suited for the binding of phosphate groups in such loops as it can adopt the required conformation to wrap the loop around the bound phosphate group [38].

For future efforts aimed at the design of inhibitors for IspE from pathogens such as *P. falciparum* or *M. tuberculosis*, the finding that the cyclopropyl substituent of ligand **15** is accommodated in the hydrophobic pocket is of particular interest (Figure 7.10b). Given that the change from Phe185 (in *E. coli* IspE) to Tyr175 (in *A. Aeolicus* IspE) increases the hydrophilicity of the small pocket, the cyclopropyl ring was not expected to be located in this subpocket as it precludes solvation of the hydroxyl group of Tyr175. This is an important finding, given that the enzymes from *P. falciparum* and *M. tuberculosis* possess a conserved tyrosine residue at this position, and that – according to homology modeling – the phenolic hydroxyl group is directed into the small pocket. The propargylic sulfonamide vector of this class of inhibitors is therefore highly suitable for precisely addressing the phenolic hydroxyl group in future design cycles.

7.4.4
Lessons Learnt from the Cocrystal Structure

By designing water-soluble inhibitors and solving the cocrystal structure of one ligand with *A. aeolicus* IspE, the suggested binding mode was validated. Thus, the first design cycle was successfully completed. The inhibitor occupies the CDP-binding pocket and exhibits a K_i value in the lower micromolar activity range. This proof of concept opens the way for further modification and optimization of the inhibitors aimed at the development of ligands with activity against IspE from medically important organisms. Thus, the cocrystal structure solved represents an important step on the way to anti-infectives with a novel mode of action.

7.5
Conclusions and Outlook

7.5.1
Conclusions

The active site of the kinase IspE features both highly polar and hydrophobic subpockets. Because the highly polar subpockets do not lend themselves well to structure-based drug design, the inhibitors were targeted to the lipophilic regions of the active site. Using structure-based design, the first inhibitors of the enzyme were developed, which display drug-like properties and highly satisfactory potency. A number of conclusions can be drawn from the series of inhibitors:

- Inhibition of IspE is possible whilst bypassing the highly polar phosphate-binding pocket in the absence of a phosphate moiety. Therefore, the ligands synthesized constitute the first potent and drug-like inhibitors of an enzyme of the nonmevalonate pathway.
- The inhibitors target only the CDP-binding pocket, potentially affording better selectivity than inhibitors designed to bind to the ATP-binding pocket.
- The majority of the binding free enthalpy is derived from the cytosine scaffold and the propargylic sulfonamide vector.
- A systematic variation of the vector's substituent provided access to SARs, confirming the proposed binding mode. In addition, these modifications gave rise to the second example of the ''55% rule'' for the optimal filling of cavities applied to an enzymatic context.
- Preparation of a water-soluble derivative enabled crystallographic studies of an enzyme–inhibitor complex, validating the proposed binding mode. This cocrystal structure provided invaluable structural information, especially in view of fine-tuning the ligands to obtain activity against the pathogenic enzymes.

In conclusion, the new target IspE revealed itself to be ideally suited to structure-based inhibitor design. The inhibitors synthesized in the context of this project represent a successful application of this design strategy.

7.5.2 Outlook

The design and synthesis of the first-generation inhibitors of IspE opened up a number of future research avenues.

First, as a result of the observed difference in amino acid sequences between the model system *E. coli* and the pathogenic enzymes – marked by the replacement of the phenylalanine residue lining the hydrophobic pocket by a tyrosine – the structure of the inhibitors will have to be fine-tuned to address this structural difference. Second, the bisubstrate approach could be tried to obtain even more potent and selective inhibitors of IspE. In principle, it should be possible to decorate the established scaffold to occupy the different pockets of the active site. Third, it would be very rewarding to identify an attractive mimic in the quest for new cytosine analogues. As opposed to the other nucleobases, very few cytosine substitutes have been described to date. Finally, identification of a generally applicable way of rendering promising inhibitors water soluble without having to undertake a time-consuming design cycle and synthesis of the new derivatives would be of great interest. In this way, attractive structures could be designed, synthesized, and assayed without worrying about their physicochemical properties such as solubility.

Acknowledgments

This work was carried out under the supervision of Prof. F. Diederich and in collaboration with the groups of Prof. A. Bacher and Prof. W. N. Hunter. Financial support by the Roche Research Foundation and the ETH Research Council is gratefully acknowledged.

List of Abbreviations

AMP-PNP	5′-adenyl-β,γ-amidotriphosphate
ATP	adenosine 5′-triphosphate
clogP	calculated partitioning coefficient
CDP	cytidine 5′-diphosphate
DMAPP	dimethylallyl diphosphate
GHMP	galactose/homoserine/mevalonate/phosphomevalonate
HTS	high-throughput screening
IC_{50}	concentration of inhibitor at which 50% maximum initial velocity is observed
IPP	isopentenyl diphosphate
IspE	4-diphosphocytidyl-2*C*-methyl-D-erythritol kinase
K_i	inhibition constant
ME	methyl-erythritol

PC	packing coefficient
PDB	protein data bank
SAR	structure–activity relationship

References

1. *http://www.cdc.gov/malaria/impact/index.htm* (accessed 23 February 2009); *http://www.cdc.gov/tb/WorldTBDay/resources_global.htm* (accessed 23 February 2009).
2. (a) Baird, J.K. (2005) Effectiveness of antimalarial drugs. *N. Engl. J. Med.*, **352**, 1565–1577; (b) Kritski, A.L., de Jesus, L.S.R., Andrade, M.K., Werneck-Barroso, E., Vieira, M.A., Haffner, A., and Riley, L.W. (1997) Retreatment tuberculosis cases. Factors associated with drug resistance and adverse outcomes. *Chest*, **111**, 1162–1167; (c) Ollé-Goig, J.E. (2006) The treatment of multi-drug resistant tuberculosis – a return to the pre-antibiotic area? *Trop. Med. Int. Health*, **11**, 1625–1628.
3. Haney, S.A., LaPan, P., Pan, J., and Zhang, J. (2006) High-content screening moves to the front of the line. *Drug Discov. Today*, **11**, 889–894.
4. Schneider, G. and Böhm, H.-J. (2002) Virtual screening and fast automated docking methods. *Drug Discov. Today*, **7**, 64–70.
5. Butler, M.S. (2004) The role of natural product chemistry in drug discovery. *J. Nat. Prod.*, **67**, 2141–2153.
6. (a) Kubinyi, H. (1998) Structure-based drug design. *Chim. Oggi*, **16**, 17–22; (b) Klebe, G. (2000) Recent developments in structure-based drug design. *J. Mol. Med.*, **78**, 269–281; (c) Van Dongen, M., Weigelt, J., Uppenberg, J., Schultz, J., and Wikström, M. (2002) Structure-based screening and design in drug discovery. *Drug Discov. Today*, **7**, 471–478.
7. Knowles, J. and Gromo, G. (2003) Target selection in drug discovery. *Nat. Rev. Drug Discov.*, **2**, 63–69.
8. (a) Bloch, K. (1992) Sterol molecule: structure, biosynthesis, and function. *Steroids*, **57**, 378–383; (b) Bochar, D.A., Friesen, J.A., Stauffacher, C.V., and Rodwell V.W. (1999)Biosynthesis of mevalonic acid from Acetyl-CoA, in *Comprehensive Natural Products Chemistry: Isoprenoids, Including Carotenoids and Steroids* (ed. D. E.Cane), Elsevier Science Publishers, Amsterdam, pp. 15–44.
9. (a) Rohmer, M., Knani, M., Simonin, P., Sutter, B., and Sahm, H. (1993) Isoprenoid biosynthesis in bacteria: a novel pathway for the early steps leading to isopentenyl diphosphate. *Biochem. J.*, **295**, 517–524; (b) Schwarz, M.K. (1994) Terpen-Biosynthese in *Gingko biloba*: Eine Überraschende Geschichte. Dissertation, ETH Zürich; (c) Broers, S.T.J. (1994) Über die Frühen Stufen der Biosynthese von Isoprenoiden in *E. coli*. Dissertation, ETH Zürich; (d) Eisenreich, W., Schwarz, M., Cartayrade, A., Arigoni, D., Zenk, M.H., and Bacher, A. (1998) The deoxyxylulose phosphate pathway of terpenoid biosynthesis in plants and microorganisms. *Chem. Biol.*, **5**, R221–R233.
10. Ruzicka, L. (1953) The isoprene rule and the biogenesis of terpenic compounds. *Experientia*, **9**, 357–367.
11. Jomaa, H., Wiesner, J., Sanderbrand, S., Altincicek, B., Weidemeyer, C., Hintz, M., Türbachova, I., Eberl, M., Zeidler, J., Lichtenthaler, H.K., Soldati, D., and Beck, E. (1999) Inhibitors of the nonmevalonate pathway of isoprenoid biosynthesis as antimalarial drugs. *Science*, **285**, 1573–1576.
12. Hunter, W.N. (2007) The nonmevalonate pathway of isoprenoid precursor biosynthesis. *J. Biol. Chem.*, **282**, 21573–21577.
13. Hirsch, A.K.H. and Diederich, F. (2008) The nonmevalonate pathway to isoprenoid biosynthesis: a potential

source of new drug targets. *Chimia*, **62**, 226–230.

14. (a) Altincicek, B., Hintz, M., Sanderbrand, S., Wiesner, J., Beck, E., and Jomaa, H. (2000) Tools for discovery of inhibitors of the 1-Deoxy-D-xylulose 5-Phosphate (DXP) synthase and DXP reductoisomerase: an approach with enzymes from the pathogenic bacterium *Pseudomonas aeruginosa*. *FEMS Microbiol. Lett.*, **190**, 329–333; (b) Mueller, C., Schwender, J., Zeidler, J., and Lichtenthaler, H.K. (2000) Properties and inhibition of the first two enzymes of the non-mevalonate pathway of isoprenoid biosynthesis. *Biochem. Soc. Trans.*, **28**, 792–793.
15. (a) Kuzuyama, T., Shimizu, T., Takahashi, S., and Seto, H. (1998) Fosmidomycin, a specific inhibitor of 1-Deoxy-D-xylulose 5-phosphate reductoisomerase in the nonmevalonate pathway for terpenoid biosynthesis. *Tetrahedron Lett.*, **39**, 7913–7916; (b) Herforth, C., Wiesner, J., Heidler, P., Sanderbrand, S., Van Calenbergh, S., Jomaa, H., and Link, A. (2004) Antimalarial activity of N6-substituted adenosine derivatives. Part 3. *Bioorg. Med. Chem.*, **12**, 755–762; (c) Walker, J.R. and Poulter, C.D. (2005) Synthesis and evaluation of 1-Deoxy-D-xylulose 5-phosphate analogues as chelation-based inhibitors of methylerythritol phosphate synthase. *J. Org. Chem.*, **70**, 9955–9959; (d) Woo, Y.H., Fernandes, R.P.M., and Proteau, P.J. (2006) Evaluation of fosmidomycin analogs as inhibitors of the Synechocystis sp PCC6803 1-Deoxy-D-xylulose 5-phosphate reductoisomerase. *Bioorg. Med. Chem.*, **14**, 2375–2385; (e) Haemers, T., Wiesner, J., Van Poecke, S., Goeman, J., Henschker, D., Beck, E., Jomaa, H., and Van Calenbergh, S. (2006) Synthesis of α-substituted fosmidomycin analogues as highly potent *Plasmodium falciparum* growth inhibitors. *Bioorg. Med. Chem. Lett.*, **16**, 1888–1891; (f) Devreux, V., Wiesner, J., Goeman, J.L., Van der Eycken, J., Jomaa, H., and Van Calenbergh, S. (2006) Synthesis and biological evaluation of cyclopropyl analogues of fosmidomycin as potent *Plasmodium falciparum* growth inhibitors. *J. Med. Chem.*, **49**, 2656–2660.
16. (a) Crane, C.M., Kaiser, J., Ramsden, N., Rohdich, F., Eisenreich, W., Hunter, W.N., Bacher, A., and Diederich, F. (2006) Fluorescent inhibitors for IspF, an enzyme in the nonmevalonate pathway for isoprenoid biosynthesis and a potential target for antimalarial therapy. *Angew. Chem.*, **118**, 1083–1087; *Angew. Chem. Int. Ed.*, **45**, 1069–1074; (b) Baumgartner, C., Eberle, C., Diederich, F., Lauw, S., Rohdich, F., Eisenreich, W., and Bacher, A. (2007) Structure-based design and synthesis of the first weak non-phosphate inhibitors for IspF, an enzyme in the nonmevalonate pathway of isoprenoid biosynthesis. *Helv. Chim. Acta*, **90**, 1043–1068.
17. (a) Reardon, J.E. and Abeles, R.H. (1986) Mechanism of action of isopentenyl pyrophosphate isomerase: evidence for a carbonium-ion intermediate. *Biochemistry*, **25**, 5609–5616; (b) Muehlbacher, M. and Poulter, C.D. (1988) Isopentenyl-diphosphate isomerase: inactivation of the enzyme with active-site-directed irreversible inhibitors and transition-state analogues. *Biochemistry*, **27**, 7315–7328; (c) Poulter, C.D., Muehlbacher, M., and Davis, D.R. (1989) Isopentenyldiphosphate isomerase. Mechanism of active-site-directed irreversible inhibition by 3-(fluoromethyl)-3-butenyl diphosphate. *J. Am. Chem. Soc.*, **111**, 3740–3742; (d) Lu, X.J., Christensen, D.J., and Poulter, C.D. (1992) Isopentenyl-diphosphate isomerase: irreversible inhibition by 3-methyl-3,4-epoxybutyl diphosphate. *Biochemistry*, **31**, 9955–9960.
18. (a) Kuzuyama, T., Takagi, M., Kaneda, K., Watanabe, H., Dairi, T., and Seto, H. (2000) Studies on the nonmevalonate pathway: conversion of 4-(cytidine 5′-diphospho)-2*C*-methyl-D-erythritol to its 2-phospho derivative by 4-(cytidine 5′-diphospho)-2*C*-methyl-D-erythritol Kinase. *Tetrahedron Lett.*, **41**, 2925–2928;

(b) Lüttgen, H., Rohdich, F., Herz, S., Wungsintaweekul, J., Hecht, S., Schuhr, C.A., Fellermeier, M., Sagner, S., Zenk, M.H., Bacher, A., and Eisenreich, W. (2000) Biosynthesis of terpenoids: YchB protein of *Escherichia coli* phosphorylates the 2-hydroxy group of 4-diphosphocytidyl-2*C*-methyl-D-erythritol. *Proc. Natl. Acad. Sci. U.S.A.*, **97**, 1062–1067.

19. Bork, P., Sander, C., and Valencia, A. (1993) Convergent evolution of similar enzymatic function on different protein folds: the hexokinase, ribokinase, and galactokinase families of sugar kinases. *Protein Sci.*, **2**, 31–40.
20. Miallau, L., Alphey, M.S., Kemp, L.E., Leonard, G.A., McSweeney, S.M., Hecht, S., Bacher, A., Eisenreich, W., Rohdich, F., and Hunter, W.N. (2003) Biosynthesis of isoprenoids: crystal structure of 4-diphosphocytidyl-2*C*-methyl-D-erythritol kinase. *Proc. Natl. Acad. Sci. U.S.A.*, **100**, 9173–9178.
21. Wada, T., Kuzuyama, T., Satoh, S., Kuramitsu, S., Yokoyama, S., Unzai, S., Tame, J.R.H., and Park, S.Y. (2003) Crystal structure of 4-(cytidine 5'-diphospho)-2*C*-methyl-D-erythritol kinase, an enzyme in the nonmevalonate pathway of isoprenoid synthesis. *J. Biol. Chem.*, **278**, 30022–30027.
22. Sgraja, T., Alphey, M.S., Ghilagaber, S., Marquez, R., Robertson, M.N., Hemmings, J.L., Lauw, S., Rohdich, F., Bacher, A., Eisenreich, W., Illarionova, V., and Hunter, W.N. (2008) Characterization of *Aquifex aeolicus* 4-diphosphocytidyl-2*C*-methyl-D-erythritol kinase – ligand recognition in a template for antimicrobial drug discovery. *FEBS J.*, **275**, 2779–2794.
23. Crane, C.M., Hirsch, A.K.H., Alphey, M.S., Sgraja, T., Lauw, S., Illarionova, V., Rohdich, F., Eisenreich, W., Hunter, W.N., Bacher, A., and Diederich, F. (2008) Synthesis and characterization of cytidine derivatives that inhibit the kinase IspE of the nonmevalonate pathway for isoprenoid biosynthesis. *ChemMedChem*, **3**, 91–101.
24. Hirsch, A.K.H., Alphey, M.S., Lauw, S., Seet, M., Barandun, L., Rohdich, F., Hunter, W.N., Bacher, A., and Diederich, F. (2008) Inhibitors of the kinase IspE: structure–activity relationships and co-crystal structure analysis. *Org. Biomol. Chem.*, **6**, 2719–2730.
25. Gerber, P.R. and Müller, K. (1995) MAB, a generally applicable molecular-force field for structure modeling in medicinal chemistry. *J. Comput.-Aided Mol. Des.*, **9**, 251–268.
26. ACD/LogP & ACD/LogD, Advanced Chemistry Development, Inc. (2005)Toronto. *www.acdlabs.com*.
27. (a) Meyer, E.A., Castellano, R., and Diederich, F. (2003) Interactions with aromatic rings in chemical and biological recognition. *Angew. Chem.*, **115**, 1244–1287; *Angew. Chem. Int. Ed.*, **42**, 1210–1250.
28. Brameld, K.A., Kuhn, B., Reuter, D.C., and Stahl, M. (2008) Small molecule conformational preferences derived from crystal structure data. A medicinal chemistry focused analysis. *J. Chem. Inf. Model.*, **48**, 1–24.
29. Hirsch, A.K.H., Lauw, S., Gersbach, P., Schweizer, W.B., Rohdich, F., Eisenreich, W., Bacher, A., and Diederich, F. (2007) Nonphosphate inhibitors of IspE protein, a kinase in the nonmevalonate pathway for isoprenoid biosynthesis and a potential target for antimalarial therapy. *ChemMedChem*, **2**, 806–810.
30. Hirsch, A.K.H. (2008) A novel approach towards antimalarials: design and synthesis of inhibitors of the kinase IspE . Dissertation, ETH Zürich.
31. Illarionova, V., Kaiser, J., Ostrozhenkova, E., Bacher, A., Fischer, M., Eisenreich, W., and Rohdich, F. (2006) Nonmevalonate terpene biosynthesis enzymes as antiinfective drug targets: substrate synthesis and high-throughput screening methods. *J. Org. Chem.*, **71**, 8824–8834.
32. Zürcher, M. and Diederich, F. (2008) Structure-based drug design: exploring the proper filling of apolar pockets at enzyme active sites. *J. Org. Chem.*, **73**, 4345–4361.

33. Zürcher, M., Gottschalk, T., Meyer, S., Bur, D., and Diederich, F. (2008) Exploring the flap pocket of the antimalarial target plasmepsin II: the ''55% Rule'' applied to enzymes. *ChemMedChem*, **3**, 237–240.

34. Mecozzi, S. and Rebek, J.Jr. (1998) The 55% solution: a formula for molecular recognition in the liquid state. *Chem. Eur. J.*, **4**, 1016–1022.

35. (a) Purse, B.W. and Rebek, J.Jr. (2006) Self-fulfilling cavitands: packing alkyl chains into small spaces. *Proc. Natl. Acad. Sci. U.S.A.*, **103**, 2530–2534; (b) Hooley, R.J. and Rebek, J.Jr. (2007) Self-complexed deep cavitands: alkyl chains coil into a nearby cavity. *Org. Lett.*, **9**, 1179–1182; (c) Gottschalk, T., Jaun, B., and Diederich, F. (2007) Container molecules with portals: reversibly switchable cycloalkane complexation. *Angew. Chem.*, **119**, 264–268; *Angew. Chem. Int. Ed.*, **46**, 260–264.

36. (2006) *Spartan'06*, Wavefunction Inc., Irvine .

37. (a) Wuitschik, G., Rogers-Evans, M., Müller, K., Fischer, H., Wagner, B., Schuler, F., Polonchuk, L., and Carreira, E.M. (2006) Oxetanes as promising modules in drug discovery. *Angew. Chem.*, **118**, 7900–7903; (b) *Angew. Chem. Int. Ed.*, **45**, 7736–7739.

38. (a) Hirsch, A.K.H., Fischer, F.R., and Diederich, F. (2007) Phosphate recognition in structural biology. *Angew. Chem.*, **119**, 342–357; *Angew. Chem. Int. Ed.*, **46**, 338–352.